Implications of Solar Magnetograms for the Drifts of Cosmic Rays

Horst Fichtner[1,2], Andreas Kopp[1,3]

(1) Institut für Theoretische Physik IV, Ruhr-Universität Bochum, Germany
(2) Res. Dept. Plasmas with Complex Interactions, RUB, Germany
(3) Centre for Space Research, North-West Univ., Potchefstroom, South Africa

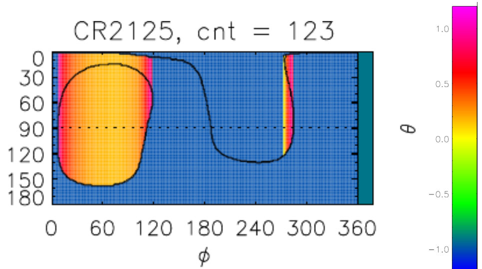

The 'topological' sign $\in [-1, +1]$ for Carr. Rot. 2125

Motivation

A **guiding question** for contemporary research activities:

Can a combination of current models of the kinetic transport of cosmic rays with magnetohydrodynamic (MHD) models of the solar wind and its turbulence be used to explain three-dimensional (3D) multi-point spacecraft data?

Example: Solar wind and energetic electron data at SOHO (black) and Ulysses (red)

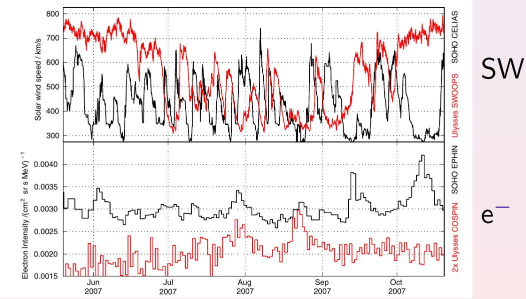

WIENGARTEN ET AL. [2014]

Motivation

A **guiding question** for contemporary research activities:

Can a combination of current models of the kinetic transport of cosmic rays with magnetohydrodynamic (MHD) models of the solar wind and its turbulence be used to explain three-dimensional (3D) multi-point spacecraft data?

Example: Solar wind and energetic electron data at SOHO (black) and Ulysses (red)

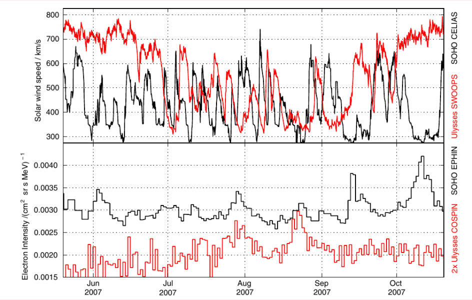

SW

e^-

WIENGARTEN ET AL. [2014]

$\longrightarrow$ ***Task: Construction of suitable combination of models***

Motivation

- Combination of MHD solar wind and kinetic cosmic ray transport models has long tradition
  (e.g., le Roux & Fichtner [1997], Guo & Florinski [2014], Kopp et al. [2017])

Motivation

- Combination of MHD solar wind and kinetic cosmic ray transport models has long tradition
  (e.g., le Roux & Fichtner [1997], Guo & Florinski [2014], Kopp et al. [2017])

- Contemporary activities include explicit modelling of solar wind turbulence and its influence on cosmic ray transport processes
  (e.g., Engelbrecht & Burger [2013], Wiengarten et al. [2016], Moloto et al. [2018])

Motivation

- Combination of MHD solar wind and kinetic cosmic ray transport models has long tradition
  (e.g., le Roux & Fichtner [1997], Guo & Florinski [2014], Kopp et al. [2017])

- Contemporary activities include explicit modelling of solar wind turbulence and its influence on cosmic ray transport processes
  (e.g., Engelbrecht & Burger [2013], Wiengarten et al. [2016], Moloto et al. [2018])

- Particularly, a physics-based modelling of (the reduction of) drifts in a structured and time-dependent solar wind that is fully consistent with observations is still missing
  (e.g., Moloto et al. [2018], Zhao et al. [2018], Kopp et al. [2021])

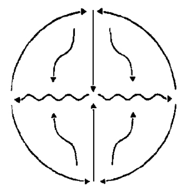

$qA > 0$

Outline of the Talk

- Introduction ($\checkmark$)
- ‘Traditional’ models of drift reduction

Outline of the Talk

- Introduction (✓)
- 'Traditional' models of drift reduction
- A new model introducing the 'topological' sign

Outline of the Talk

- Introduction (✓)
- ‘Traditional’ models of drift reduction
- A new model introducing the ‘topological’ sign
- Résumé

Traditional models of drift reduction

Heliospheric particle drifts are described by

$$\langle \mathbf{v}_\mathrm{d} \rangle = \nabla \times \left(\kappa_\mathrm{A} \frac{\mathbf{B}}{B} \right) \quad ; \quad \kappa_A = qA\kappa_{\mathrm{A},0} \frac{P\beta}{3B} \frac{(P/P_0)^2}{1+(P/P_0)^2} \quad ; \quad \kappa_{\mathrm{A},0} \in [0,1]$$

Traditional models of drift reduction

Heliospheric particle drifts are described by

$$\langle \mathbf{v}_\mathrm{d} \rangle = \nabla \times \left(\kappa_\mathrm{A} \frac{\mathbf{B}}{B} \right) \quad ; \quad \kappa_A = q A \kappa_{\mathrm{A},0} \frac{P\beta}{3B} \frac{(P/P_0)^2}{1+(P/P_0)^2} \quad ; \quad \kappa_{\mathrm{A},0} \in [0,1]$$

Reduction Method I:

Phenomenological coupling to (current sheet) tilt angle α:

$$\kappa_{\mathrm{A},0} = \left[\cos\left(\frac{\pi}{150^\circ} \alpha \right) \right]^{\frac{\alpha}{c_1}}$$

Ferreira & Potgieter [2003], Raath [2019]

Traditional models of drift reduction

Heliospheric particle drifts are described by

$$\langle \mathbf{v}_\mathrm{d} \rangle = \nabla \times \left(\kappa_\mathrm{A} \frac{\mathbf{B}}{B} \right) \quad ; \quad \kappa_A = qA\kappa_{\mathrm{A},0} \frac{P\beta}{3B} \frac{(P/P_0)^2}{1+(P/P_0)^2} \quad ; \quad \kappa_{\mathrm{A},0} \in [0,1]$$

Reduction Method I:

Phenomenological coupling to (current sheet) tilt angle α:

$$\kappa_{\mathrm{A},0} = \left[\cos\left(\frac{\pi}{150^\circ} \alpha \right) \right]^{\frac{\alpha}{c_1}}$$

Ferreira & Potgieter [2003], Raath [2019]

Reduction Method II:

Direct coupling to turbulence δB:

$$\kappa_{\mathrm{A},0} = \left(1 + \frac{{\lambda_\perp}^2}{{R_\mathrm{L}}^2} \frac{\delta B^2}{B^2} \right)^{-1}$$

Engelbrecht et al. [2017], Moloto et al. [2018]

Traditional models of drift reduction

Heliospheric particle drifts are described by

$$\langle \mathbf{v}_\mathrm{d} \rangle = \nabla \times \left(\kappa_\mathrm{A} \frac{\mathbf{B}}{B} \right) \quad ; \quad \kappa_A = qA\kappa_{\mathrm{A},0} \frac{P\beta}{3B} \frac{(P/P_0)^2}{1+(P/P_0)^2} \quad ; \quad \kappa_{\mathrm{A},0} \in [0,1]$$

Reduction Method I:

Phenomenological coupling to (current sheet) tilt angle α:

$$\kappa_{\mathrm{A},0} = \left[\cos\left(\frac{\pi}{150^\circ} \alpha \right) \right]^{\frac{\alpha}{c_1}}$$

Ferreira & Potgieter [2003], Raath [2019]

Reduction Method II:

Direct coupling to turbulence δB:

$$\kappa_{\mathrm{A},0} = \left(1 + \frac{{\lambda_\perp}^2}{{R_\mathrm{L}}^2} \frac{\delta B^2}{B^2} \right)^{-1}$$

Engelbrecht et al. [2017], Moloto et al. [2018]

<u>Problems</u>: parametrization with α too simple; $\delta B/B$ exhibits only weak, if any, dependence on solar cycle

A new model models of drift reduction

Heliospheric particle drifts are described by

$$\langle \mathbf{v}_\mathrm{d} \rangle = \nabla \times \left(\kappa_\mathrm{A} \frac{\mathbf{B}}{B} \right) \quad ; \quad \kappa_A = qA\kappa_{\mathrm{A},0} \frac{P\beta}{3B} \frac{(P/P_0)^2}{1+(P/P_0)^2} \quad ; \quad \kappa_{\mathrm{A},0} \in [0,1]$$

New Reduction Method:

Coupling to topology of magnetic field maps (see figure):

$$A \to \sigma_\mathrm{t} \mathrel{\hat{=}} \text{‘topological’ sign}$$

KOPP ET AL. [2021]

- $A = \pm 1$ discrete
- $\sigma_\mathrm{t} \in [-1, 1]$ continuous

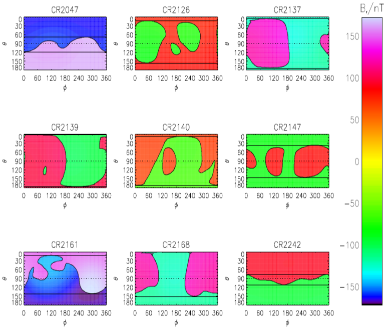

A new model models of drift reduction

Heliospheric particle drifts are described by

$$\langle \mathbf{v}_\mathrm{d} \rangle = \nabla \times \left(\kappa_\mathrm{A} \frac{\mathbf{B}}{B} \right) \quad ; \quad \kappa_A = qA\kappa_{\mathrm{A},0} \frac{P\beta}{3B} \frac{(P/P_0)^2}{1+(P/P_0)^2} \quad ; \quad \kappa_{\mathrm{A},0} \in [0,1]$$

New Reduction Method:

Coupling to topology of magnetic field maps (see figure):

$A \to \sigma_\mathrm{t} \mathrel{\hat{=}}$ 'topological' sign

Kopp et al. [2021]

- $A = \pm 1$ discrete
- $\sigma_\mathrm{t} \in [-1, 1]$ continuous

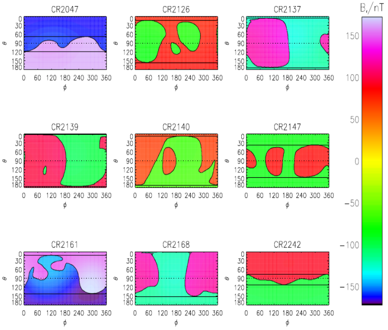

Advantage: *allows for localized regions with ordered drift motion and is using the MHD boundary conditions*

Computation of the topological sign

- **Step 0**: Computation of magnetic field maps from GONG maps (WIENGARTEN ET AL. [2014]: potential field assumption)

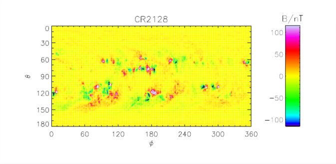

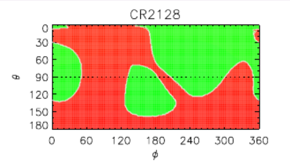

Computation of the topological sign

- **Step 0**: Computation of magnetic field maps from GONG maps (WIENGARTEN ET AL. [2014]: potential field assumption)

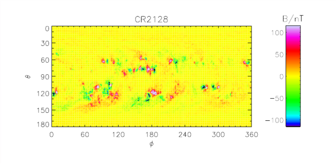

$\longrightarrow$

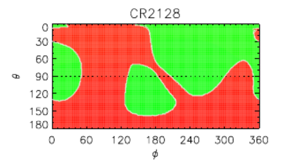

- **Step 1**: New determination of tilt angle(s) from the magnetic field maps, i.e. latitudes of heliospheric current sheet

  $\rightarrow$ new tilt angles can be greater than Wilcox tilt angles which are limited to ± 75 deg

Computation of the topological sign

- **Step 0**: Computation of magnetic field maps from GONG maps (Wiengarten et al. [2014]: potential field assumption)

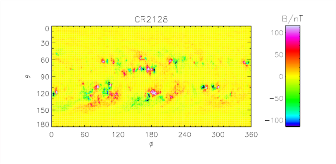

$\longrightarrow$

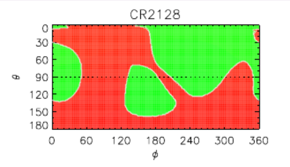

- **Step 1**: New determination of tilt angle(s) from the magnetic field maps, i.e. latitudes of heliospheric current sheet

  $\rightarrow$ new tilt angles can be greater than Wilcox tilt angles which are limited to $\pm 75\,\mathrm{deg}$

- **Step 2**: Computation of topological sign $\sigma_{\mathrm{t}} \in [-1, +1]$ that takes into account localized regions of opposite field polarities

Step 1: New vs. Wilcox tilt angles

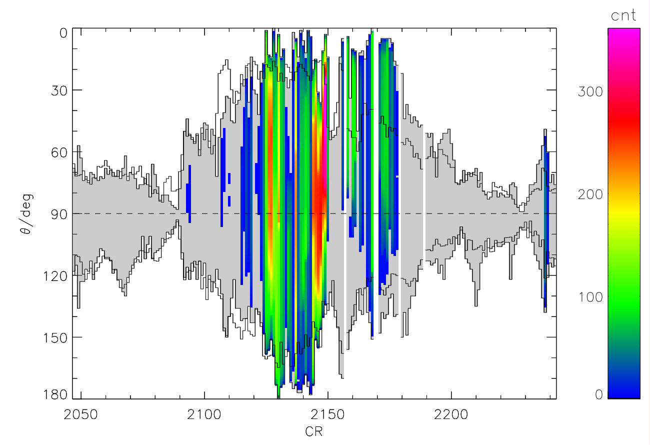

- new angles: gray area, thick lines
- WSO angles: thin lines
- colored bars: extent of region with multiple HCS crossings

Step 2: Topological sign

Distinguish sign of 'inner' and 'outer' regions (Kopp et al. [2021]):

$$\sigma_\mathrm{t} = \langle \sigma_\mathrm{t,out}(\varphi) + w(\varphi)\sigma_\mathrm{t,inn}(\varphi)\rangle_\varphi \; ; \; w(\varphi) = (\tilde{\vartheta}_\mathrm{max}(\varphi) - \tilde{\vartheta}_\mathrm{min}(\varphi))/180^\circ$$

with

$$\sigma_\mathrm{t,out}(\varphi) = \frac{1}{2}\left(q_\mathrm{r}(\tilde{\vartheta}_\mathrm{min}(\varphi) - 1, \varphi) - q_\mathrm{r}(\tilde{\vartheta}_\mathrm{max}(\varphi) + 1, \varphi)\right)$$

and

$$q_\mathrm{r}(\vartheta, \varphi) \quad = \quad \frac{B_\mathrm{r}(\vartheta, \varphi)}{|B_\mathrm{r}(\vartheta, \varphi)|}$$

($\sigma_\mathrm{t,inn}$ similar, see ICRC paper)

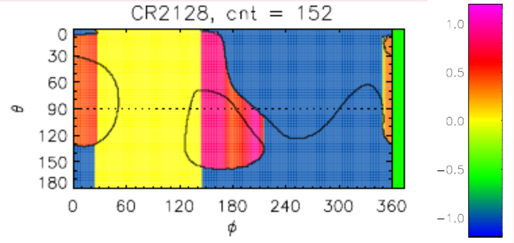

Step 2: Topological sign vs. Carrington Rotation

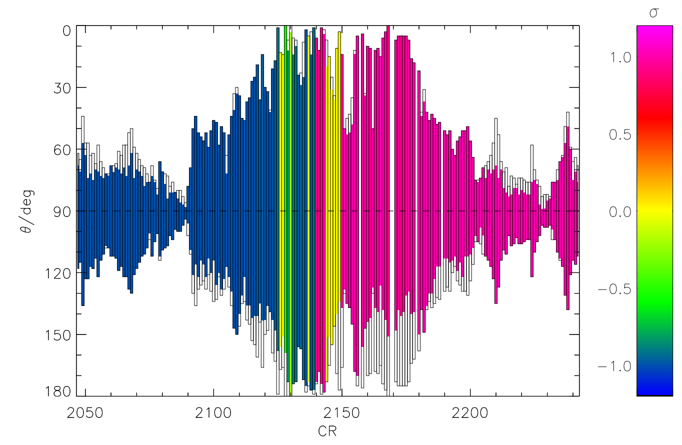

- new tilt angles with topological sign
- box extensions indicate mirrored larger value of other hemisphere
- sign of the cycle changes between CRs 2139 and 2140

Résumé

The **topological sign**

- *generalizes previous approaches, which were limited to* $A = \pm 1$*, to* $\sigma_{\mathrm{t}} \in [-1, +1]$
- *takes into account the topology of magnetic field maps at the heliobase and is, thus, explicitly physics-based (as opposed to heuristic)*
- *enables a consistent coupling of kinetic transport and MHD models in the sense that they are employing the same boundary conditions*
- *approach may be supplemented by additional effects due to, e.g., turbulence*